Journal of Electrochemistry

Volume 28
Issue 3 *Special Issue: Frontier of Electrochemistry (Ⅱ)*

2022-03-28

An Additive Incorporated Non-Nucleophilic Electrolyte for Stable Magnesium Ion Batteries

Mao-Ling Xie

Jun Wang

Chen-Ji Hu

Lei Zheng

Hua-Bin Kong

Yan-Bin Shen

Hong-Wei Chen
1. College of Materials Science and Engineering, Huaqiao University, Xiamen 361021, Fujian, China;,
hwchen@hqu.edu.cn

See next page for additional authors

Recommended Citation

Mao-Ling Xie, Jun Wang, Chen-Ji Hu, Lei Zheng, Hua-Bin Kong, Yan-Bin Shen, Hong-Wei Chen, Li-Wei Chen. An Additive Incorporated Non-Nucleophilic Electrolyte for Stable Magnesium Ion Batteries[J]. *Journal of Electrochemistry*, 2022 , 28(3): 2108561.
DOI: 10.13208/j.electrochem.210856
Available at: https://jelectrochem.xmu.edu.cn/journal/vol28/iss3/1

An Additive Incorporated Non-Nucleophilic Electrolyte for Stable Magnesium Ion Batteries

Authors

Mao-Ling Xie, Jun Wang, Chen-Ji Hu, Lei Zheng, Hua-Bin Kong, Yan-Bin Shen, Hong-Wei Chen, and Li-Wei Chen

Corresponding Author(s)

Hong-Wei Chen(hwchen@hqu.edu.cn);
Li-Wei Chen(lwchen2008@sinano.ac.cn)

电 化 学
J. Electrochem. 2022, 28(3), 2108561 (1 of 8)

[Article] DOI: 10.13208/j.electrochem.210856 Http://electrochem.xmu.edu.cn

An Additive Incorporated Non-Nucleophilic Electrolyte for Stable Magnesium Ion Batteries

Mao-Ling Xie[1,3#], Jun Wang[1#], Chen-Ji Hu[2,3], Lei Zheng[3], Hua-Bin Kong[1], Yan-Bin Shen[3], Hong-Wei Chen[1*], Li-Wei Chen[2,3*]

(*1. College of Materials Science and Engineering, Huaqiao University, Xiamen 361021, Fujian, China; 2. In-Situ Center for Physical Science, School of Chemistry and Chemical Engineering, Shanghai Jiaotong University, Shanghai 200240, China; 3. i-Lab, Suzhou Institute of Nano-Tech and Nano-Bionics, Chinese Academy of Science, Suzhou 215123, Jiangsu, China*)

Abstract: Non-nucleophilic electrolytes are promising next-generation highly stable electrolytes for magnesium-ion batteries (MIBs). However, a passivation layer on Mg metal anode usually blocks Mg^{2+} diffusion, leading to poor reaction kinetics and low Coulombic efficiency of the Mg plating/stripping in these electrolytes. Here we explore the utilization of phenyl disulfide (PDF) as a film-forming additive for non-nucleophilic electrolytes to regulate the interfacial chemistry on Mg metal anode. Phenyl-thiolate generated from the PDF additive was found to suppress the unfavorable surface blocking layer, resulted in a high Coulombic efficiency of up to 99.5% for the Mg plating/stripping process as well as a remarkably decreased overpotential. The full battery consisting of Mg metal anode and Mo_6S_7Se cathode remained stable in the PDF additive-containing electrolyte at 0.1 C over 150 cycles at room temperature.

Key words: magnesium-ion batteries; non-nucleophilic electrolyte; interface; additives; phenyl disulfide

1 Introduction

The energy densities of traditional lithium-ion batteries (LIBs) are approaching an inherent limit set by the intrinsic properties of electrode materials[1-3]. Rechargeable magnesium-ion batteries (MIBs) using magnesium (Mg) metal anode have been investigated as a promising alternative to LIBs since Mg metal is relatively inexpensive, safe, and delivers nearly twice as much volumetric capacity as lithium (Li) metal anode (3833 $mAh\cdot cm^{-3}$ vs. 2046 $mAh\cdot cm^{-3}$)[4-6]. An important advantage of Mg metal is that it does not form dendrites during long-term plating/stripping, which suggests that MIBs may potentially be employed as high-safety battery systems[7,8]. However, the widespread application of MIBs has been held back due to a lack of practically reliable electrolytes[9-11].

Practically desirable MIB electrolytes, in general, should meet the following requirements: (1) suitable for reversible Mg plating/stripping on Mg metal, (2) highly effective in Mg^{2+} conduction within a wide voltage window, and (3) high thermal stability and low toxicity. The key challenge lies in the growth of a Mg^{2+} non-conducting layer on Mg anode in conventional electrolytes due to the strong reducibility of Mg metal[8,12]. A family of nucleophilic organometallic electrolytes, known as dichloro complex electrolyte

Cite as: Xie M L, Wang J, Hu C J, Zheng L, Kong H B, Shen Y B, Chen H W, Chen L W. An additive incorporated non-nucleophilic electrolyte for stable magnesium ion batteries. *J. Electrochem.*, 2022, 28(3): 2108561.

Received: 2021-12-28, Revised: 2022-01-20. # Xie M L and Wang J contributed equally to this work. *Corresponding author, Hong-Wei Chen: Tel: (86-592)6162251, E-mail: hwchen@hqu.edu.cn, Li-Wei Chen: Tel: (86-21)54743179, E-mail: lwchen2018@sjtu.edu.cn

(DCC), were first developed in early 2000s to solve the problem[4]. DCC is obtained through the reaction of Lewis acid R_nAlCl_{3-n} (R = alkyl, aryl) with Lewis base R_mMgCl_{2-m} and is chemically inert to Mg metal, and thus enables effective Mg plating/stripping without generating the Mg^{2+} blocking passivation layer. However, DCC based nucleophilic electrolyte suffers from limited electrochemical stability window (ESW), high cost, toxicity, and sensitivity to oxidation[13]. Furthermore, the Lewis acid used for the preparation of DCC is recognized as a source of contamination, which may cause co-deposition of Al^{3+} and Mg^{2+} species, and thus greatly shortened the lifespan of these organometallic electrolytes[14].

On the other hand, non-nucleophilic electrolytes consisting of organic-salts and ether solvents integrate the merits of DCC with relatively wide ESW, low toxicity and facile preparation[15-17]. Besides, the Lewis acid-free non-nucleophilic electrolytes prevent the unfavorable Mg^{2+}-Al^{3+} from co-deposition. More importantly, non-nucleophilic electrolytes can be extended to Mg/organics or Mg/sulfur batteries that cannot be operated in DCC electrolytes[18-20]. However, because of the strong reducibility of Mg metal, the dissolved Mg salts, solvents or even a trace amount of impurities in the electrolyte will inevitably react with Mg metal and generate an ion blocking passivation layer[10], resulting in poor Mg plating/stripping efficiency and slow kinetics for MIBs. Therefore, the challenge for non-nucleophilic electrolytes is to tailor the structure and ion-conducting properties of the passivation layer on Mg metal anode[21-23].

Here we explore the potential of phenyl disulfide (PDF) as a film-forming additive for the regulation of Mg anode interfacial chemistry. A non-nucleophilic electrolyte consisting of magnesium hexamethyldisilazide ($Mg(HMDS)_2$) and ether solvent was selected as the model electrolyte, and the additive incorporated electrolyte is termed as P-HMDS. Benefiting from the built-in weak disulfide bond, PDF molecules are split into two phenyl thiolate anions during electrochemical cycling[24,25]. With the assistance of these intermediate species, an organic interfacial layer was generated *in-situ*, and it suppressed the growth of passivation layer on the Mg metal. As a result, the overpotential of Mg plating/stripping operated in this P-HMDS electrolyte was drastically reduced to ~ 41 mV, and the Coulombic efficiency (CE) was as high as 99.5% after 170 cycles at 1 $mA \cdot cm^{-2}$. This additive incorporated non-nucleophilic electrolyte significantly extended the cycle life of MIBs. The work provides a convenient approach to develop non-nucleophilic electrolytes towards practical MIBs.

2 Experimental

2.1 Chemicals and Materials

Magnesium bis(hexamethyldisilazido) ($Mg(HMDS)_2$, > 97%) was purchased from Aladdin. $MgCl_2$ (99.99%) and Mg metal (99.5%) were purchased from Sigma-Aldrich. Phenyl disulfide (PDF, 98%+) was purchased from Adamas. Electrolytes were purchased from Guangzhou Tinci Materials Technology Corporation, China. Mo_6S_7Se was synthesized according to the reference[26].

2.2 Sample Synthesis and Characterizations

0.3 $mol \cdot L^{-1}$ $Mg(HMDS)_2$ and 1.2 $mol \cdot L^{-1}$ $MgCl_2$ were dissolved in anhydrous tetrahydrofuran (THF) solvent as the blank electrolyte. 0.01 $mol \cdot L^{-1}$, 0.025 $mol \cdot L^{-1}$, 0.05 $mol \cdot L^{-1}$ and 0.1 $mol \cdot L^{-1}$ phenyl disulfid (PDF) were separately dissolved into the blank electrolyte to prepare different P-HMDS electrolytes. The Mg metal sheets were thoroughly polished three times with sandpaper to remove the oxide layer, then rinsed with THF (extra dry with molecular sieves, water ⩽ 30 ppm, in resealable bottle) prior to use. The polished Mg metals were utilized within 1 min to assemble the cells in a glovebox to minimize possible oxidation of the Mg surface. For the full cell, Mo_6S_7Se was used as the cathode and glass fiber membrane was used as the separator. The amount of electrolyte used is estimated to be 120 μL for each cell. The cells were discharged and charged on a battery test system (CT-3008-5V, NEWARE technology Ltd. Shenzhen). The ionic conductivity of each group of electrolytes was tested using a LEICI DDS-307A conductivity meter, and the amount of electrolyte was

6 mL. CV experiment was carried out with a sweep rate of 0.5 mV·s^{-1} and between 0 to 2.0 V (vs. Mg^{2+}/Mg, Biologic VMP 300) at room temperature of 25 ℃.

The sample was characterized by a field emission SEM (Hitachi Regulus8230) at 5.0 KV. The GC/MS measurements were performed using Agilent 7890B/5977A GC/MSD instrument (Agilent Technologies Co., Ltd.). The X-ray photoelectron spectroscopic (XPS) data was collected used PHI-5000 VersaProbe (Al K_α radiation). Prior to XPS characterization, anhydrous THF was used to rinse the samples which were prepared in a glove box filled with an argon gas. The NMR measurements were performed at room temperature (~ 25 ℃). The FTIR spectra were collected using a Thermoscientific Nicolet 6700 spectrometer.

3 Results and Discussion

PDF was added into 0.3 mol·L^{-1} $Mg(HMDS)_2$ electrolyte with different concentrations from 0.01 to 0.1 mol·L^{-1}, yielding a series of homogeneous P-HMDS electrolytes. The ionic conductivity of the P-HMDS increased from 9.1 × 10^{-4} to 1.2 × 10^{-3} S·cm^{-1} when the concentration of PDF increased from 0 (blank) to 0.05 mol·L^{-1} (Figure 1(A)). Further increase in PDF concentration leads to reduction in ionic conductivity. The addition of the PDF additive, which contains no Mg^{2+}, may still affect the ionic conductivity of the electrolyte via mechanisms such as changes in solvation structure or coordination sites, which will be topics of future studies.

The effect of the PDF additive on Mg plating/stripping overpotentials was firstly investigated in symmetric Mg cells where the galvanostatic cycling was performed under 1 mA·cm^{-2} with a capacity of 0.5 mAh·cm^{-2}. As shown in Figure 1(B) and (C), the control cell with no PDF exhibited a large overpotential of ~ 92 mV after 100-h cycling. With the addition of 0.01 mol·L^{-1} PDF, the overpotential after the same 100-h cycling slightly declined to ~ 68 mV. The overpotential further decreased to ~ 41 mV with the increased PDF concentration of 0.05 mol·L^{-1}, less than half that of the control cell. Even after 800-h of continuous galvanostatic cycling in the P-HMDS with 0.05 mol·L^{-1} PDF, the symmetric Mg cell showed no evidence of failure (Figure 1(D), (E)), suggesting that 0.05 mol·L^{-1} PDF is the optimal concentration that enables a stable utilization of Mg metal anode. More

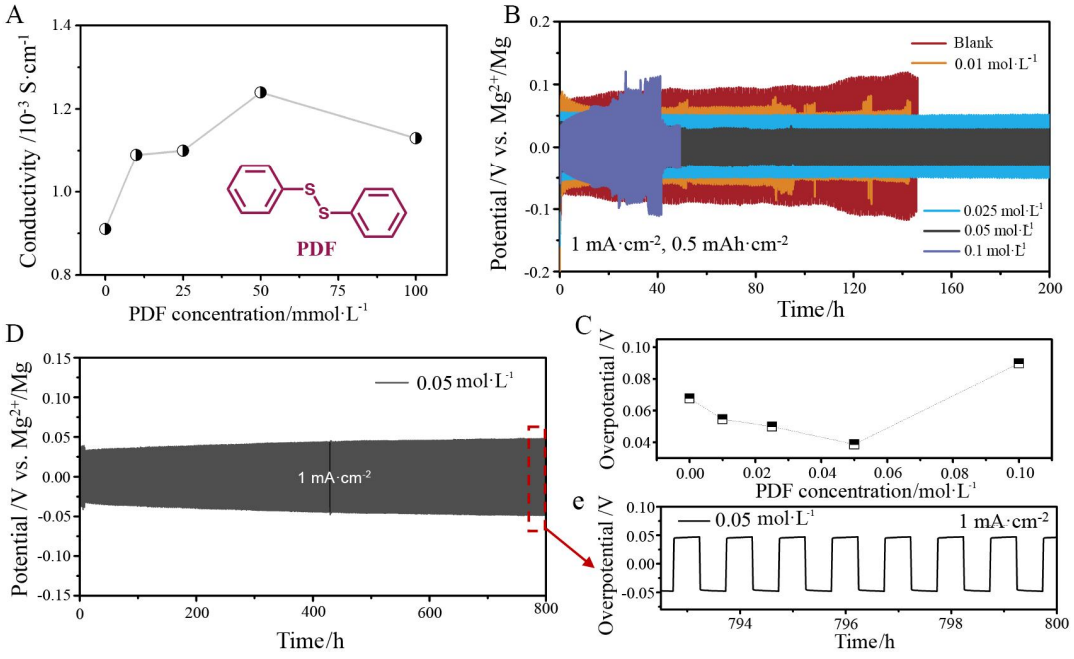

Figure 1 (A) Ion conductivities of P-HMDS with different PDF concentrations. (B) Plating/stripping of Mg/Mg cell in P-HMDS with different PDF concentrations. (C) The corresponding overpotentials of the Mg/Mg cells. (D) Long-term plating/stripping of Mg/Mg cell in P-HMDS with 0.05 mol·L^{-1} PDF. (E) The expanded view from the plating/stripping curve in (D). (color on line)

attention was thus focused on the P-HMDS with 0.05 mol·L^{-1} PDF in the following studies.

To further evaluate the electrolytes, asymmetric Mg/SS (stainless steel) cells were assembled to investigate the corresponding CE values of the Mg plating/stripping behavior. In each cycle, 0.5 mAh·cm^{-2} of Mg metal was deposited on the SS substrate at 1 mA·cm^{-2}, and then stripped until the voltage reached 1 V vs. Mg^{2+}/Mg. The CE of Mg plating/stripping can be obtained by comparing the amounts of Mg removed from and deposited on the substrate. As shown in Figure 2(A), the 1st CE of the Mg/SS cell with 0.05 M PDF was 91.7%, and the cell can be stably cycled for more than 150 cycles with a high average CE of 99.5%. In contrast, the 1st CE of the PDF-free Mg/SS control cell was only ~ 67.7%. It means that about one-third of Mg deposition cannot be stripped from the SS electrode during charging, which may be due to the unfavorable side reaction on the Mg metal. The CE of the control cell with no PDF increased slowly in the initial 60 cycles and exhibited a large variation with a low average value of only 96.9%.

In addition, the plating/stripping overpotentials within different electrolytes varied greatly. As shown in Figure 2(B), the overpotential in P-HMDS (~ 112 mV) was lower than that in the baseline electrolyte (~ 164 mV), suggesting the optimized plating/stripping kinetics in the P-HMDS electrolyte. Another notable difference is that, in the P-HMDS, a voltage jump was observed until the stripping process reached closer to the end, while in the baseline electrolyte, the stripping voltage started to rise when only three quarters of Mg metal were stripped from the SS substrate (Figure 2(B)). It suggests that some non-active or poorly conductive components existed on the electrode in the baseline electrolyte, resulting in a large energy barrier that retards Mg stripping out of the electrode. This is also confirmed by the impedance evolution of the symmetrical Mg/Mg cells. In line with the large plating/stripping overpotential in the baseline electrolyte, the cell shows a typical symmetric semicircle, corresponding to a large interfacial resistance of ~ 5.8 kΩ after 50 cycles (Figure 2(C)). In contrast, for the cell using P-HMDS, the Nyquist curve turned into asymmetric, suggesting a newly formed interface on Mg metal (Figure 2(D)). Meanwhile, the corresponding overall resistance decreased to ~ 350 Ω after 50 cycles, one order of magnitude lower than that of the baseline electrolyte, which is also in line with the decreased overpotential of the corresponding cell using P-HMDS. To shed further understanding into the plating/stripping process, the

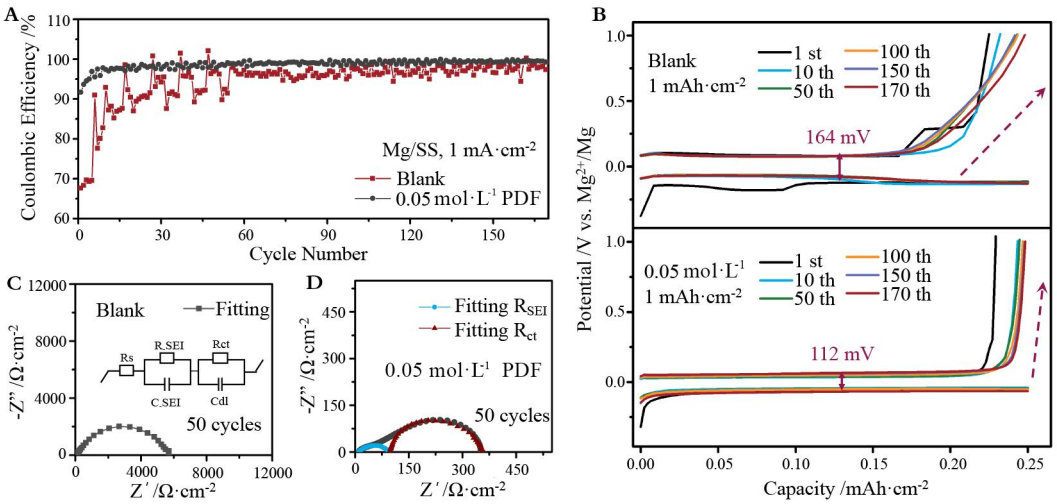

Figure 2 (A) Coulombic efficiency (CE) of plating/stripping on a SS working electrode in the P-HMDS with or without 0.05 mol·L^{-1} PDF at current density of 1 mA·cm^{-2}. (B) Voltage curves of the corresponding Mg/SS cells. (C-D) EIS curves of Mg/Mg cells after 50 cycles in (C) blank electrolyte and (D) P-HMDS with 0.05 mol·L^{-1} PDF at 1 mA·cm^{-2}. Inset in (C) shows the equivalent circuit used to fit the EIS data.(color on line)

Nyquist curve was fitted into two semicircles corresponded to ion diffusion in the interface (i.e., interfacial resistance, R_{SEI}) and the charge transfer on Mg metal (R_{ct}). For the symmetric Mg/Mg cells, the R_{SEI} on either side of the symmetric Mg metal electrode can be determined by dividing the total R_{SEI} into two and then normalized to the surface area of Mg metal. The R_{SEI} values of Mg metal were found to be ~2.9 k$\Omega\cdot$cm^2 and 50 $\Omega\cdot$cm^2 for the cells without and with 0.05 mol$\cdot$L^{-1} PDF additive, respectively. That is, an optimized interfacial process where the Mg^{2+} diffusion through the surface layer is facilitated by adding PDF into the $Mg(HMDS)_2$ electrolyte.

The improved kinetics may be attributed to the PDF-assisted conductive interfacial layer on Mg metal. This assumption is reasonable as the PDF molecules possess weak -S-S- bonds with low dissociation energy. Thus, they can easily be electrochemically reduced into thiophenolate anions (TP^-) on the electrode surface[25,27]. That was confirmed by using gas chromatography-mass spectrometry (GC-MS) to monitor the evolution of the electrolyte components. As shown in Figure S1 in SI, a newly formed TP^- species emerged, and the content of the TP^- anions slightly increased with cycling time. We speculate that the nucleophilic TP^- anions could adsorb on the metal surface in the form of TP-Mg (schematically shown in the inset of Figure 3(A)), in a fashion similar to that of the well-known self-assembly of thiol molecules on Au substrate via Au-S bonds[28]. XPS analysis confirms this hypothesis. To ensure removals of physisorbed salt and other species on Mg metal, all the collected Mg metals were thoroughly rinsed with tetrahydrofuran solvent before each XPS measurement. As shown in the S 2p spectrum of the Mg metal cycled in PDF-free electrolyte, basically no S signal was observed after the 100th cycle (Figure 3 (A)). In comparison, however, a significant S 2p signal appeared in the Mg metal from the P-HMDS case, which can be ascribed to typical phenyl thiolate (TP) derivates[29]. That is also in well agreement with the GC-MS analysis. Since only the PDF molecules contain elemental S in the cell, these S-containing species on the Mg metal must come from the decomposition of PDF additive. As the surface of Mg metal had been thoroughly cleaned, the TP^- is not physisorbed on the Mg electrode, but probably existed in the form similar to coordination bonds[30,31].

Importantly, the growth of the passivation layer on Mg metal is thus significantly repressed by the new interfacial process, which can also be confirmed from the Mg 2p spectrum of XPS results. In the baseline electrolyte, inorganic Mg salts were observed on the surface of Mg metal, including MgO and MgCO that are widely considered as poor Mg^{2+} conductors (Figure 3(A)), which formed the typical passivation layer on the Mg metal. In the P-HMDS electrolyte, however, the contents of MgO and $MgCO_3$ were significantly reduced without generating new inorganic Mg salts on the Mg surface. Moreover, consistent with the S 2p spectrum (Figure 3(B)), new organic-Mg species on the Mg metal arising from the TP^- bonding were found based on the Mg 2p spectrum (Figure 3(B)). Consequently, benefiting from the hopping sites on the TP species (comes from the lone pair electrons on elemental S), the resulted organic-rich interface may thus provide more convenient pathways to promote fast Mg^{2+} diffusion toward the Mg metal, which explains the improved interfacial kinetics of Mg^{2+} as discussed above[32,33].

Benefitting from the PDF-assisted interfacial chemistry, a denser and smoother Mg deposition was also observed in the P-HMDS electrolyte, as shown in the SEM images in Figure 3(B)&(C). In general, the typical Mg deposition in non-nucleophilic electrolytes is moss-like covered with a passivated crust that formed when its surface is in contact with electrolytes. In contrast, the deposited Mg metal in the P-HMDS have a smoother surface with smaller particle sizes and size distribution more evenly on the electrode surface. This smooth deposition surface could also be attributed the preferential adsorption of TP- on the Mg surface, in a way similar to self-assembled monolayers[34], which would result in fast and homogeneous Mg deposition. Schematic illustration of the interfacial process with/without PDF is shown

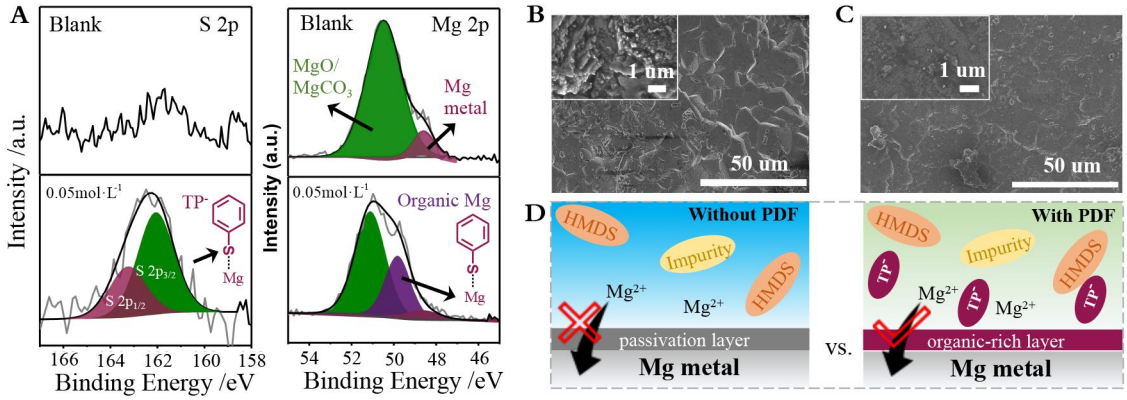

Figure 3 (A) XPS results(S 2p and Mg 2p scan) of Mg/Mg cells after 100th cycling in P-HMDS with/without 0.05mol·L^{-1} PDF at 1 mA·cm^{-2}. (B-C) The corresponding morphologies evolution of Mg anode after 100th cycling in (B) blank P-HMDS and (C) P-HMDS with 0.05 mol·L^{-1} PDF at 1 mA·cm^{-2}. (D) Schematic illustration of TP- species bonding on the Mg anode and generating the conductive layer to prevent Mg anode passivation. (color on line)

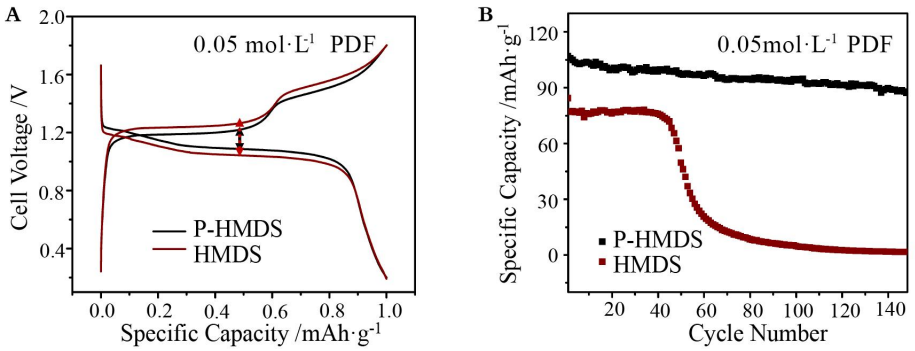

Figure 4 (A) The normalized first charge/discharge curves of Mg/Mo_6S_7Se full cell in the electrolytes with/without 0.05 mol·L^{-1} PDF at 0.1 C (1 C = 128 mA·cm^{-2}). (B) The corresponding cycling performance curves of the full cells. (color on line)

in Figure 3(D).

From the above discussion it is clear that the PDF additive significantly promotes the electrochemical reaction kinetics on Mg metal. Full batteries composed of Mo_6S_7Se cathode and Mg-metal anode were assembled to further test the practical applicability of the PDF additive. Figure 4(A) shows the normalized discharge/charge curves of the batteries cycling in different electrolytes. The voltage hysteresis of the Mg/Mo_6S_7Se battery in P-HDMS was significantly reduced, from ~ 200 mV in the PDF-free electrolyte to ~ 120 mV in the P-HDMS electrolyte. Furthermore, the cells with PDF incorporated electrolytes exhibited better specific capacity of the cathode and much prolonged cycle life. The first discharge specific capacities were 103 (with PDF) and 86 mAh·g^{-1} (without PDF) at 0.1 C. The capacity of the control battery without PDF additive faded rapidly after only ~ 40 cycles (Figure 4(B)), which is mainly ascribed to the increasing polarization on the Mg metal anode. On the contrary, the cell with P-HMDS was cycled more than 150 cycles under the same current condition, with a low capacity fade rate of 0.08% per cycle. It also showed the stable cycling response over 270 cycles at 2 C (Figure S3). In short, the battery using P-HMDS electrolyte exhibited the decreased overpotential as well as the improved cycling stability.

4 Conclusions

In summary, this work investigated the PDF as an additive for Mg metal anode. The PDF molecule contains a weak disulfide bond, which would be dis-

socia ted upon electrochemical cycling at Mg metal anode. The resulting TP^- intermediates would then tightly bond to the Mg metal surface and suppress the growth of ion blocking layer that is rich in inorganic components such as MgO and Mg_2CO_3. Significantly enhanced interfacial kinetics on the Mg metal was thus realized with the help of this organic-rich surface, leading to a remarkably decreased Mg plating/stripping overpotential to ~ 41 mV with a high CE of 99.5%. The PDF-incorporated $Mg(HMDS)_2$ electrolyte enabled more than 150 cycles for the Mg/Mo_6S_7Se full battery with a low capacity fade rate of only 0.08% per cycle, along with a decreased overpotential. This work sheds light to construct a stable and Mg^{2+} conductive surface while suppressing the passivation layer on the Mg metal operated in other electrolytes.

Acknowledgements:

This work was financially supported by the National Natural Science Foundation of China (21625304), the Natural Science Foundation of Fujian Province (2019J06018) and the Natural Science Foundation of Xiamen, China (3502Z20206008).

References:

[1] Goodenough J, Kim Y. Challenges for rechargeable Li batteries[J]. Chem. Mater., 2010, 22(3): 587-603.

[2] Li M, Lu J, Chen Z W, Amine K. 30 years of lithium-ion batteries[J]. Adv. Mater., 2018, 30(33): 1-24.

[3] Dusastre V. Materials for sustainable energy: A Collection of peer-reviewed research and review articles from nature publishing group[M]. World Scientific, 2010.

[4] Aurbach D, Lu Z, Schechter A, Gofer Y, Gizbar H, Turgeman R, Cohen Y, Moshkovich M, Levi E. Prototype systems for rechargeable magnesium batteries[J]. Nature, 2000, 407: 724-727.

[5] Niu J, Zhang Z, Aurbach D. Alloy anode materials for rechargeable Mg ion batteries[J]. Adv. Energy Mater., 2020, 10(23): 1-33.

[6] Choi J, Aurbach D. Promise and reality of post-lithium-ion batteries with high energy densities[J]. Nat. Rev. Mater., 2016, 1(4): 1-16.

[7] Aurbach D, Gofer Y, Lu Z, Schechter A, Chusid O, Gizbar H, Cohen Y, Ashkenazi V, Moshkovich M, Turgeman R. A short review on the comparison between Li battery systems and rechargeable magnesium battery technology[J]. J. Power Sources, 2001, 97-98: 28-32.

[8] Attias R, Salama M, Hirsch B, Goffer Y, Aurbach D. Anode-electrolyte interfaces in secondary magnesium batteries[J]. Joule, 2019, 3(1): 27-52.

[9] Mohtadi R, Mizuno F. Magnesium batteries: Current state of the art, issues and future perspectives[J]. Beilstein J. Nanotechnol., 2014, 5(1): 1291-1311.

[10] Deivanayagam R, Ingram B , Shahbazian-Yassar R. Progress in development of electrolytes for magnesium batteries[J]. Energy Storage Mater., 2019, 21: 136-153.

[11] Muldoon J, Bucur C B, Oliver A G, Sugimoto T, Matsui M, Kim H S, Allred G D, Zajicek J, Kotani Y. Electrolyte roadblocks to a magnesium rechargeable battery [J]. Energy Environ. Sci., 2012, 5(3): 5941-5950.

[12] Shi J, Zhang J, Guo J, Lu J. Interfaces in rechargeable magnesium batteries[J]. Nanoscale Horiz., 2020, 5(11): 1467-1475.

[13] Li Y, Guan S, Huo H, Ma Y, Gao Y, Zuo P, Yin G. A review of magnesium aluminum chloride complex electrolytes for Mg batteries[J]. Adv. Funct. Mater., 2021, 31 (24): 1-22.

[14] Liu F, Wang T, Liu X, Fan L Z. Challenges and recent progress on key materials for rechargeable magnesium batteries[J]. Adv. Energy Mater., 2021, 11(2): 1-28.

[15] Wang F F, Guo Y S, Yang J, Nuli Y, Hirano S I. A novel electrolyte system without a Grignard reagent for rechargeable magnesium batteries[J]. Chem. Commun., 2012, 48 (87): 10763-10765.

[16] Shuai H, Xu J, Huang K. Progress in retrospect of electrolytes for secondary magnesium batteries[J]. Coord. Chem. Rev., 2020, 422: 213478.

[17] Zhao-Karger Z, Zhao X, Fuhr O, Fichtner M. Bisamide based non-nucleophilic electrolytes for rechargeable magnesium batteries[J]. RSC Adv., 2013, 3(37): 16330-16335.

[18] Mao M, Gao T, Hou S, Wang C S. A critical review of cathodes for rechargeable Mg batteries[J]. Chem. Soc. Rev., 2018, 47(23): 8804-8841.

[19] Tan S, Xiong F, Wang J, An Q, Mai L Q. Crystal regulation towards rechargeable magnesium battery cathode materials[J]. Mater. Horiz., 2020, 7(8): 1971-1995.

[20] Kim H S, Arthur T S, Allred G D, Zajicek J, Newman J G, Rodnyansky A E, Oliver A G, Boggess W C, Muldoon J. Structure and compatibility of a magnesium electrolyte with a sulphur cathode[J]. Nat. Commun., 2011, 2 (1): 1-6.

[21] Xu K. Electrolytes and interphases in Li-ion batteries and

beyond[J]. Chem. Rev., 2014, 114(23): 11503-11618.

[22] Sun Y, Zou Q, Wang W, Lu Y C. Non-passivating anion adsorption enables reversible magnesium redox in simple non-nucleophilic electrolytes[J]. ACS Energy Lett., 2021, 6(10): 3607-3613.

[23] Li X, Gao T, Han F, Ma Z, Fan X, Hou S, Eidson N, Li W, Wang C. Reducing Mg anode overpotential via ion conductive surface layer formation by iodine additive[J]. Adv. Energy Mater., 2018, 8(7): 1-6.

[24] Wu M, Bhargav A, Cui Y, Siegel A, Agarwal M, Ma Y, Fu Y. Highly reversible diphenyl trisulfide catholyte for rechargeable lithium batteries[J]. ACS Energy Lett., 2016, 1(6): 1221-1226.

[25] Pipes R, Bhargav A, Manthiram A. Phenyl disulfide additive for solution-mediated carbon dioxide utilization in Li-CO_2 batteries[J]. Adv. Energy Mater., 2019, 9(21): 1-8.

[26] Aurbach D, Suresh GS, Levi E, Mitelman A, Mizrahi O, Chusid O, Brunelli M. Progress in rechargeable magnesium battery technology[J]. Adv. Mater., 2007, 19(23): 4260-4267.

[27] Roux M V, Foces-Foces C, Notario R, Ribeiro da Silva M A, Ribeiro da Silva M, Santos A, Juaristi E. Experimental and computational thermochemical study of sulfur-containing Amino acids: L-Cysteine, L-Cystine, and L-Cysteine-derived radicals. S-S, S-H, and C-S bond dissociation enthalpies[J]. J. Phys. Chem. B, 2010, 114(32): 10530-10540.

[28] Scheriber F. Structure and growth of self-assembling monolayers[J]. Prog. Surf. Sci., 2000, 65(5-8): 151-257.

[29] Roberts J, Friend C. Spectroscopic identification of surface phenyl thiolate and benzyne on Mo(110)[J]. J. Chem. Phys., 1988, 88(11): 7172-7180.

[30] Lu J Y, Ke C Z, Gong Z L, Li D P, Ci L J, Zhang L, Zhang Q B. Application of *in-situ* characterization techniques in all-solid-state lithium batteries[J]. Acta Phys. Sin., 2021, 70(19): 198102.

[31] Zhang Q B, Gong Z L, Yang Y. Advance in interface and characterizations of sulfide solid electrolyte materials. Acta Phys. Sin., 2020, 69(22): 228803.

[32] Yang K, Chen L, Ma J, Lai C, Huang Y, Mi J, Biao J, Zhang D, Shi P, Xia H. Stable interface chemistry and multiple ion transport of composite electrolyte contribute to ultra-long cycling solid-state $LiNi_{0.8}Co_{0.1}Mn_{0.1}O_2$/lithium metal batteries[J]. Angew. Chem. Int. Ed., 2021, 60: 24668-24675.

[33] Lei D, He Y B, Huang H, Yuan Y, Zhong G, Zhao Q, Hao X, Zhang D, Lai C, Zhang S. Cross-linked beta alumina nanowires with compact gel polymer electrolyte coating for ultra-stable sodium metal battery[J]. Nat. Comm., 2019, 10: 1-11.

[34] Yi R W, Mao Y Y, Shen Y B, Chen L W. Self-assembled monolayers for batteries[J]. J. Am. Chem. Soc., 2021, 143 (33): 12897-12912.

基于非亲核电解液构建稳定的镁离子电池

谢茂玲[1,3#],王 钧[1#],胡晨吉[2,3],郑 磊[3],孔华彬[1],沈炎宾[3],陈宏伟[1*],陈立桅[2,3*]

(1. 华侨大学材料科学与工程学院,福建 厦门 361021; 2. 上海交通大学,物质科学原位中心,化学化工学院,上海 200240; 3. 中国科学院苏州纳米技术与纳米仿生研究所 i-Lab,江苏 苏州 215123)

摘要: 非亲核电解液被认为是新一代可用于镁离子电池的高稳定电解液。但由于电解液容易在镁金属表面产生不传导镁离子的钝化层,导致镁的电化学沉积/溶出过程在该电解液中表现出动力学缓慢、库仑效率较低等缺点。在本研究中,我们通过在非亲核电解液中引入二苯二硫醚(PDF)添加剂以实现对镁金属电极的界面调控。研究表明 PDF 产生的苯基硫醇盐中间体可以紧密结合在镁金属表面,并显著抑制了镁金属表面钝化层的生成。经界面优化后的镁金属电极的沉积-溶出库仑效率高达 99.5%,并且表现出显著降低的过电位。利用此电解液,并以镁金属为负极、Mo_6S_7Se 为正极构建的镁离子电池在室温下可稳定循环 150 周(0.1 C)。这类通过添加剂优化镁金属界面的策略也将有助于推进其他类型的镁离子电解液的实际应用。

关键词: 镁离子电池;非亲核电解质;电极界面;添加剂;二苯二硫醚